ACADEMIA ROMÂNĂ
Revue Roumaine de Chimie
http://web.icf.ro/rrch/

Rev. Roum. Chim.,
2011, *56*(8), 833-841

PRO206SER AND ARG441HIS MUTATIONS INFLUENCE ON HUMAN TRYPTOPHAN HYDROXYLASE 2 ACTIVITY – A MOLECULAR MODELING STUDY

Maria MERNEA, Octavian CĂLBOREAN, Andrei TIȚA and Dan Florin MIHAILESCU*

University of Bucharest, Faculty of Biology, Department of Anatomy, Animal Physiology and Biophysics, 91-95 Splaiul Independentei, Bucharest, 050095, Roumania

Received December 20, 2010

Tryptophan hydroxylase (TPH) catalyzes the rate limiting reaction in the biosynthesis of the neurotransmitter serotonin. In the brain, serotonin production is controlled by tryptophan hydroxylase 2 (TPH2). Two TPH2 mutations have been linked to serotoninergic pathology: Pro206Ser, associated with the bipolar disorder and Arg441His, associated with major depression. We investigated the influence of these two mutations on the catalytic site architecture and on the flexibility of the TPH2 monomer using molecular modeling techniques. The architecture of the catalytic site with ferric iron was derived from quantum mechanics techniques. According to our results, the two mutations alter TPH2 functionality by widening and increasing the solvation energy of the catalytic site. Normal modes analysis of wt and mutant TPH2 revealed that mutation increase the flexibility of the regulatory domain and of the cofactor binding region. The influence of phosphorylations was also taken into account.

INTRODUCTION

Tryptophan hydroxylase (TPH) is a tetrahydrobiopterin-dependent aromatic amino acid hydroxylase, along with tyrosine hydroxylase and phenylalanine hydroxylase. TPH catalyzes the first, rate-limiting reaction of the serotonin synthesis pathway, namely it converts L-tryptophan to 5-hydroxytriptophan.[1] The neurotransmitter serotonin mediates behaviors like mood, aggressivity, anxiety, appetite, sleep.[2, 3] Disturbances of the serotoninergic system are associated with psychiatric disorders clustered in unipolar major depression and bipolar (BP) disorder.[4, 5]

Two isoforms of TPH are present in the human body: TPH1and TPH2. The two isoforms have different tissue specificity, enzyme kinetics (TPH1 presents a lower K_M value) and regulatory features, including different phosphorylation sites.[6] TPH1 is expressed in the non-neural serotoninergic tissues (the enterochromaffin cells of the intestine, the pineal gland and skin, where it is involved in melatonin synthesis), while TPH2 is specific for the neural serotoninergic tissues (central nervous system and enteric neurons). TPH1 and TPH2 are encoded by two different genes, localized on the chromosomes 11 (TPH1) and 12 (TPH2).[7] As TPH2 is the brain-specific isoform of tryptophan hydroxylase, it has been the focus of genetic association studies addressing the relationship between the mutations in TPH2 and affective disorders.[8, 9]

TPH2 is a homotetramer. Each monomer is catalytically active and comprises three functional regions: a regulatory N-terminal region, a catalytic domain and the tetramerization C-terminal domain.[10] Like in all other aromatic amino acid hydroxylases, the catalytic site of TPH2 comprises iron coordinated by two histidines (His318 and His 323) and one carboxylate (Glu363).[11,12] This iron coordination motif is present in all mononuclear non-heme iron(II) enzymes.[13] TPH2 is activated by protein kinase A that phosphorylates the enzyme at Ser19 and Ser104.[14] Two other putative phosphoryla-

* Corresponding author: dan.mihailescu@bio.unibuc.ro

tion sites were identified,[15] but their functional role was not confirmed by experiments.

Two TPH2 mutations have been linked to serotoninergic pathology: Pro206Ser (a mutation localized in the sixth exon of *tph2* gene, SNP rs11178997), associated with BP disorder and Arg441His (the polymorphism of a single nucleotide G1463A), associated with major depression.[16,17] TPH2 harboring the mutation Pro206Ser has a similar catalytic activity as wtTPH2, but has a decreased solubility and thermal stability. The mutation Arg441His alters the catalytic activity, solubility and thermal stability at a greater extent than Pro206Ser. When wt TPH2 is expressed with either Pro206Ser or Arg441His, the final TPH2 activity is significantly reduced. This phenomenon can be caused by heterotetramer destabilization caused by the unstable mutant monomers.[9]

We investigated the mechanism by which mutations alter the functionality of TPH2 by using molecular modeling techniques. The analysis was conducted on structural models of wt and mutant TPH2 monomers (with mutations Pro206Ser and Arg441His) built based on the homology with tyrosine and phenylalanine hydroxylases. We considered the situation when only the cofactor Fe^{3+} and three water molecules are present in the catalytic site. The spatial arrangement of the catalytic site with iron in the ferric state was derived from hybrid quantum mechanics-molecular mechanics calculations. We addressed the questions of the how the catalytic site surface and solvation energy changes in the mutant monomers and how the flexibility of the monomers is affected by mutations. We modeled the phosphorylations at all the putative sites present in our models and determined their influence on the catalytic site electrostatic features and on the wt and mutant monomers flexibility.

MATERIALS AND METHODS

Wt TPH2 models

We used BLAST[18] server to identify the proteins with known structures and amino acids sequences similar with that of TPH2. We identified several biopterin-dependent hydroxylase structures with catalytic sites harboring different substrates or co-substrates.[11,12,19-21] The structural model of tetrameric TPH2 was built mainly based on the known structure of chicken tryptophan hydroxylase 1 (pdb code: 3e2t[11]). The C-terminal ACT domain was built using rat phenylalanine hydroxylase (pdb code:1phz[19]). For modeling the tetramerization region we identified two templates: human phenylalanine hydroxylase (pdb code: 2pah[20]) and rat tyrosine hydroxylase (pdb code: 1toh[21]). Therefore, taking into account both folding possibilities for the tetramerization region, we built two models of TPH2: TPH2-F with a loose folding as in phenylalanine hydroxylase and TPH2-Y with a tight folding, as in tyrosine hydroxylase. TPH2 structures were modeled using MODELLER[22] based on the sequence alignments with the templates above stated. The catalytic site was modeled only with iron in the ferric state and three water molecules, using as template the catalytic site of human phenylalanine hydroxylase (pdb code: 1pah[23]). The monomers of the two structures are very similar, having a root mean squared deviation of 1.1 Å between their whole backbones. Therefore we decided to perform further calculation only on one of them, namely one monomer from our TPH2-F model. TPH2-F monomer will be further termed TPH2 monomer.

Quantum mechanics/molecular mechanics simulations

We used quantum mechanics/molecular mechanics methods in order to minimize the energy of one TPH2-F monomer with Fe^{3+} and three water molecules positioned in the catalytic site. The region treated using quantum mechanics was restricted to the catalytic site of the monomer that comprises the three residues involved in Fe^{3+} coordination (His318, His323 and Glu363), the Fe^{3+} ion and the three water molecules. The rest of the monomer was treated using the molecular mechanics techniques provide by the software CHARMM.[24] Quantum mechanics calculations were performed using the ab initio quantum chemistry package GAMESS.[25] We used Restricted Open-Shell Hartree-Fock (ROHF) level of theory with basis set 6-31G*. The energy minimization consisted of 1000 minimization steps using an adopted basis Newton-Raphson method (ABNR).

Coordinated Fe^{3+} simulation parameters specific for TPH2

The QM/MM energy minimized TPH2-F monomer was analyzed and the spatial arrangement

of Fe^{3+} coordinated by the three TPH2 residues was determined by measuring the distances and angles between Fe^{3+} and the two Nε2 atoms of His318 and His 323 and the Oα2 atom of Glu363. The results were integrated into a new patch that creates bonds between Fe^{3+} and the atoms that coordinate it. The length of the bonds and the angle values were set to the values measured in the equilibrated structure. The force constants for bonds and angles were set to the values of similar bonds and angles found in heme structure (the topology and parameters of heme are integrated in CHARMM force field[26]). Simulations performed using this new patch have proved that the spatial arrangement of Fe^{3+}, the three water molecules and the three residues that coordinate iron is conserved, even after a great number of minimization steps (data not shown).

Phosphorylated and mutant TPH2 models

The phosphorylation sites present in our TPH2 models are: Ser104, Ser382 and Ser392. Based on the monomer of TPH2 energetically optimized by QM/MM calculations, we modeled the phosphorylations using CHARMM. Mutant TPH2 monomers comprising the mutations Pro206Ser and Arg441His have been modeled based on the QM/MM equilibrated structure using CHARMM. These monomers were phosphorylated using the same protocol as for wt.

Normal modes analysis (NMA)

All the TPH2 monomer structures (wt and expressing the mutations Pro206Ser or Arg441His, both phosphorylated and unphosphorylated) have been rigorously energy minimized in order to be suited for applying the harmonic approximation and to generate the normal modes of vibration. Energy minimization was performed for the number of steps (using both Steepest Descent and Adopted Basis Newton-Rhapson algorithms) required to generating vibration modes with positive frequencies. Energy minimization was performed with CHARMM.[24] NMA was performed using the VIBRAN[24, 27] module in CHARMM.

We analyzed the catalytic site of the energetically minimized structures for which the normal modes analysis outputted only positive frequencies in order to determine the effect of mutations and phosphorylation. The catalytic site was considered to be the proteic region within 5 Å of Fe^{3+} and water molecules. The solvent accessible surface (SAS) of the catalytic site was calculated as the surface accessible to a probe radius of 1.4 Å. The electrostatic surface energy (EPE) was calculated using PBEQ module[28] from CHARMM[24] using a grid centered in the center of the catalytic site, with a minimum distance between the solute and the grid boundary of 10 Å and a coarse grid spacing of 1.5 Å before focusing and 1 Å after focusing. For the dielectric boundary, we considered the molecular contact and reentrant surface created using the water radius (1.4 Å) and the atomic radii of protein atoms found in CHARMM force field. We calculated the catalytic site EPE in water (EPE 80) by using a protein dielectric constant of 1, a bulk-solvent dielectric constant of 80 and a salt concentration of 0.15 M/L, at 310 K. We further calculated the EPE value in a reference environment (EPE 1) by using a bulk-solvent dielectric constant of 1. The solvation free energy (E solv) of the catalytic site was calculated as the difference between the electrostatic surface potential energy of the structure in water and the electrostatic surface potential energy in a reference environment, with a dielectric constant of 1.

RESULTS AND DISCUSSION

TPH2 catalytic site

The QM/MM equilibrated TPH2 monomer structure reveals a symmetric arrangement of the catalytic site in which the Fe^{3+} ion is found at similar distances from the protein and water atoms that coordinate it. Also, after the QM/MM energy minimization, the angles formed by Fe^{3+} and the atoms that coordinate it are equalized and have values close to 90^{o}. The catalytic site with iron in the ferric state is represented in Fig. 1. The values for bonds measured between Fe^{3+} and the atoms that coordinate it are also displayed in Fig. 1.

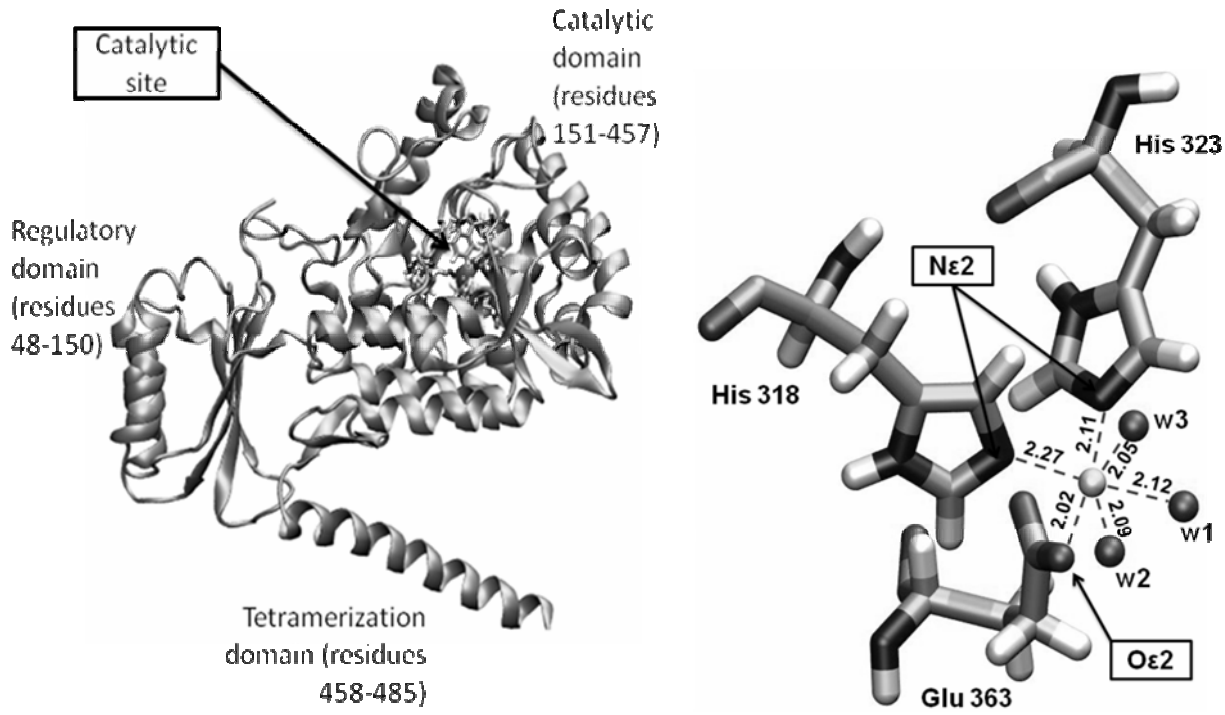

Fig. 1 – The wt TPH2 monomer structure as derived from the QM/MM calculations is presented in the left section of the figure. The functional domains and the catalytic site location are labeled. The catalytic site arrangement is provided in the right section of the figure. The residues that coordinate iron (His318, His323 and Glu363) are represented as licorice. The atoms involved in coordinating iron are also labeled. Fe^{3+} is represented as a yellow sphere and the oxygen atoms of the three water molecules (w1, w2 and w3) from the catalytic site are represented as red spheres. Distances measured between Fe^{3+} and the atoms that coordinate it after QM/MM energy minimization are reported.

TPH2 catalytic site in wt and mutant monomers

In order to characterize and compare the catalytic site of wt TPH2 monomer with the catalytic sites of monomers harboring one of the mutations Pro206Ser or Arg441 His, both without and with phosphorylations, we evaluated its hydrophobic properties as a function of the solvent accessible surface (SAS) and its solvation free energy (E solv).[29]

The solvent accessible surface (SAS) of the catalytic site is involved in defining the hydrophobic term of the interaction with the substrate and co-substrates. Results presented in Table 1 show that, in the case of unphosphorylated monomers, the catalytic site of wt TPH2 presents the smallest SAS value. The mutant monomers present wider catalytic sites, Arg441His TPH2 having the largest SAS value. In the case of phosphorylated wt TPH2, SAS does not change upon phosphorylation. In contrast, the SAS value in phosphorylated Pro206Ser TPH2 increases with ~150 $Å^2$, while SAS value for phosphorylated Arg441His decreases with ~40 $Å^2$.

Table 1

Solvent accessible surface (SAS), electrostatic potential energy in water (EPE 80) and in a reference environment (EPE 1) and the solvation energy (E Solv) of the catalytic site of wt TPH2, Pro206Ser TPH2 and Arh441His TPH2 monomers, in both unphosphorylated and phosphorylated states

Structure	SAS ($Å^2$)	EPE 80 (kcal/ mol)	EPE 1 (kcal/ mol)	E Solv (kcal/ mol)	Phosphorylated structure	SAS ($Å^2$)	EPE 80 (kcal/ mol)	EPE 1 (kcal/ mol)	E Solv (kcal/ mol)
wtTPH2	1076	1638	1659	-20	wtTPH2	1077	3073	3123	-50
Pro206Ser	1101	1283	1324	-42	Pro206Ser	1249	3556	3674	-118
Arg441His	1129	1315	1377	-62	Arg441His	1092	1364	1421	-57

The reaction catalyzed by TPH2 involves Fe^{3+} desolvation in order to allow substrate and co substrate binding in the catalytic site. In the case of the mutant monomers, the solvation energies calculated for the catalytic sites are increased relative to the wt monomer, with Arg441His TPH2 having the largest solvation energy. Large solvation energy in this area creates a high energetic barrier for the reaction with the consequence of a lower enzymatic activity.[30] Based on our data, in the unphosphorylated state, Arg441His TPH2 has a lower enzymatic activity than Pro206Ser TPH2 and both of them have a lover activity than wt. These results are in agreement with the available mutagenesis data on wt and mutant TPH2.

In the case of phosphorylated monomers, the catalytic site of Pro206Ser TPH2 monomer presents solvation energy ~2-fold higher than the solvation energy of the catalytic site in Arg441His TPH2 and wt. Phosphorylation is expected to activate the enzyme;[14] therefore we would have expected the catalytic sites of phosphorylated structures to have more favorable solvation energies than the unphosphorylated ones. We observed a decrease in the catalytic site solvation energy only in the case of phosphorylated Arg441His TPH2. In the case of wt and Pro206Ser TPH2, the solvation energy of the catalytic site is significantly increased. The phosphorylation sites present in our TPH2 model are Ser104, Ser382 and Ser392. Among them, only the functional role of Ser104 has been confirmed by enzyme kinetics experiments.[14] According to our model, Ser382 is found very close to the catalytic site (distance between Fe^{3+} and Ser382 is 5 Å). By modeling the phosphorylation at this site, we added a high negative charge (2 elementary charges) close to the catalytic site. The disagreement between data obtained for the phosphorylated and unphosphorylated structures suggests that we should reconsider the phosphorylated TPH2 models.

TPH2 monomers flexibility

We addressed the flexibility of wt and mutant TPH2 monomers, in both unphosphorylated and phosphorylated states by performing normal modes analysis. We calculated and analyzed the 100 lowest modes generated using normal modes analysis as they are expected to reveal the collective conformational changes relevant for wt and mutant TPH2 monomers functionality. Wt TPH2 alpha carbons (Cα) fluctuations in the lowest normal mode (the first non-zero frequency normal mode) are presented in Fig. 2 as a function of amino acids sequence. The highest displacements correspond to the N-terminal region of the monomer, which represents the regulatory domain of TPH2. Their high fluctuations are not surprising, as the regulatory domain represents a source of hTPH2 instability and reduced solubility.[10]

In order to compare the differences between the fluctuations of mutant and phosphorylated TPH2 with the fluctuation of wt TPH2 Cα atoms, we calculated their relative fluctuations as percentages of wt TPH2 Cα atoms fluctuations. In Fig. 2 (b)-(f) are presented the relative fluctuations of mutant TPH2 and phosphorylated mutant and wt TPH2. The peaks seen on these plots correspond to regions significantly displaced relative to wt TPH2. Values of 100% correspond to regions with identical fluctuations as wt. The flexibility of phosphorylated wt TPH2 is significantly increased for residues 158-176 (400%), residues 325-346 (210%), residues 48-69 (180%) and for residues 278-297 (150%). The residues 416-443 are less flexible in phosphorylated wt TPH2 (40%).

In the case of Pro206Ser TPH2, significant high relative fluctuations are seen in residues 50-67 (330%), 158-194 (2000%), 266-300 (250%) and 322-343 (800%). Significant low relative fluctuations are seen in the case of residues 418-435 (12%). In the phosphorylated Pro206Ser TPH2 monomer we identified only high relative fluctuations regions: 50-67 (250%), 153-174 (5500%), 184-205 (250%), 330-346 (1100%), 359-377 (150%) and 412-441 (1000%).

The highest relative fluctuations of Arg441His TPH2 are localized in the regions comprised between residues 50-67 (700%), 160-177 (8000%), 281-297 (400%), 324-340 (1100%), 366-378 (250%) and 422-428 (550%). In the phosphorylated Arg441His TPH2, the same regions as in the unphosphorylated structure present high relative fluctuations, as follows: 50-67 (570%), 160-177 (5800%), 281-297 (350%), 324-340 (850%), 366-378 (200%) and 422-428 (420%).

In the slowest normal mode, both mutations and phosphorylation alter the flexibility of regions between residues 50-67, 158-177, 325-340 and 418-435. The region between residues 50-67 is part of the regulatory domain of TPH2, a s source of instability in wt TPH2.[10] The increased fluctuations of this region in mutant TPH2 models and in phosphorylated wt and mutant TPH2 should account for an increased instability of the mutant monomers relative to wt, with Arg441His TPH2 being the most unstable.

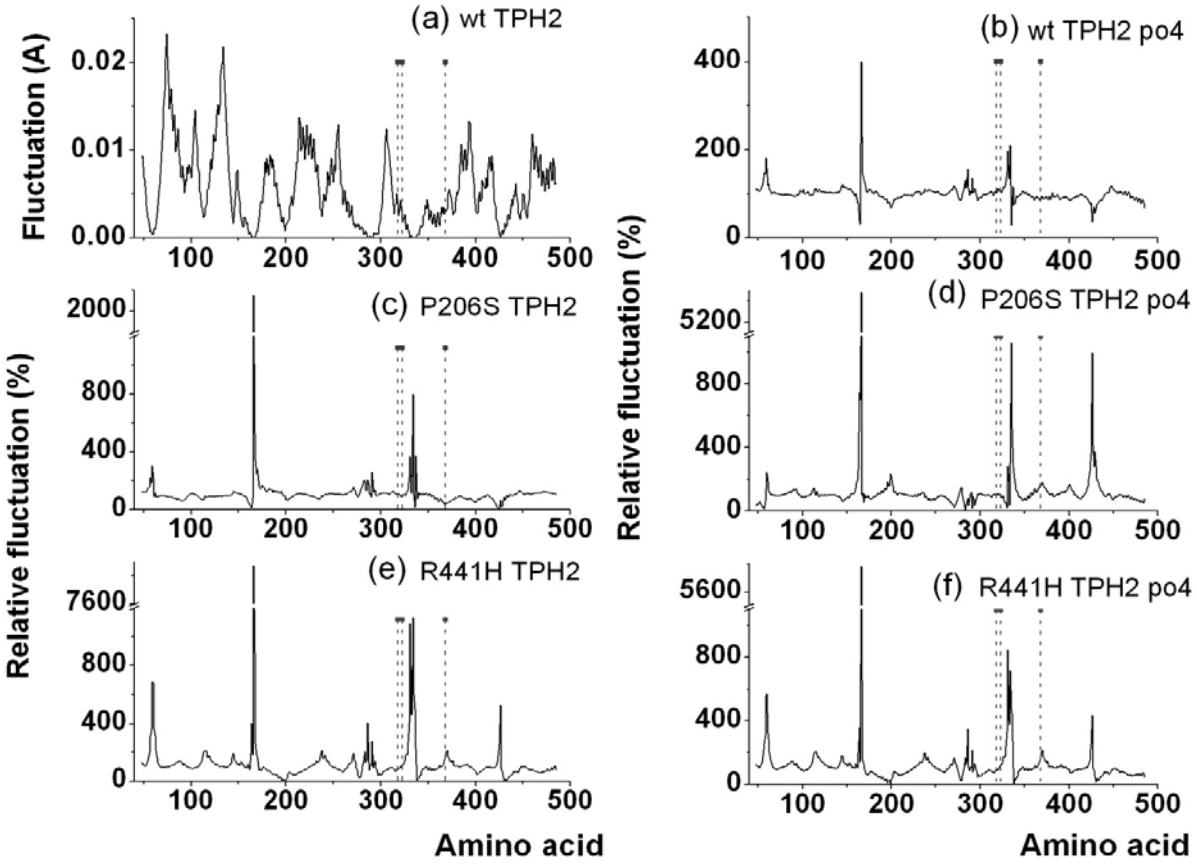

Fig. 2 – (a) The fluctuations of Cα atoms from wt TPH2 monomer during the lowest normal mode. (b),(c),(d),(e),(f) The relative fluctuations of phosphorylated wt TPH2 (b), Pro206Ser TPH2 (c), phosphorylated Pro206Ser TPH2 (d), Arg441His TPH2 (e)and phosphorylated Arg441His TPH2 (f). The relative fluctuations were calculated by dividing the fluctuations of Cα atoms from the considered structures to the fluctuations of Cα atoms from wt TPH2 times 100. In all the plots, residues involved in iron coordination are marked with "▪".

Residues 158-177 comprise a cofactor binding region (residues 169-175 [12]). Relative to wt TPH2, the flexibility of this region is increased in mutant TPH2, while the flexibility of the loops lining the active site (residues 309-315 and 409-418 [12]) is constant. These differences should account for the altered enzymatic activity of TPH2 harboring mutations. The presence of phosphorylations also increases the flexibility of the cofactor binding region in wt, but to a smaller extent than in the mutant unphosphorylated models. The influence of phosphorylations studied on our fully phosphorylated models does not appear to be consistent with enzyme activation, as phosphorylations increase the catalytic site solvation energy (results presented in the previous section) and also increase the flexibility of cofactor binding region. A more systematic analysis is required for establishing the influence of phosphorylations.

In our structural TPH2 models, residues 325-340 and 418-435 are spatially close. Both of the regions are spatially close to residue 441. These residues are found at 22 Å (in the case of residues 325-340) and 36 Å (in the case of residues 418-435) distance from residue 206. In the unphosphorylated state, Pro206Ser increases only the flexibility of residues 325-340, while in the phosphorylated state, it affects both regions, with a significant effect on the flexibility of the remote 418-435 region. Arg441His alters the flexibility of the two regions in both phosphorylated and unphosphorylated states.

Correlated motions of TPH2

In order to understand the effect of mutations on the correlated and anticorrelated motions of TPH2 monomer during the slowest normal mode, we present the covariance matrix of all Cα atoms pairs in Fig. 3. The strongest positive correlations between residues corresponds to the correlation values greater than 0.8, while the strongest negative correlations correspond to values smaller than -0.8. Residues with correlation values greater than -0.2 and smaller than 0.2 are considered to move independently.[31]

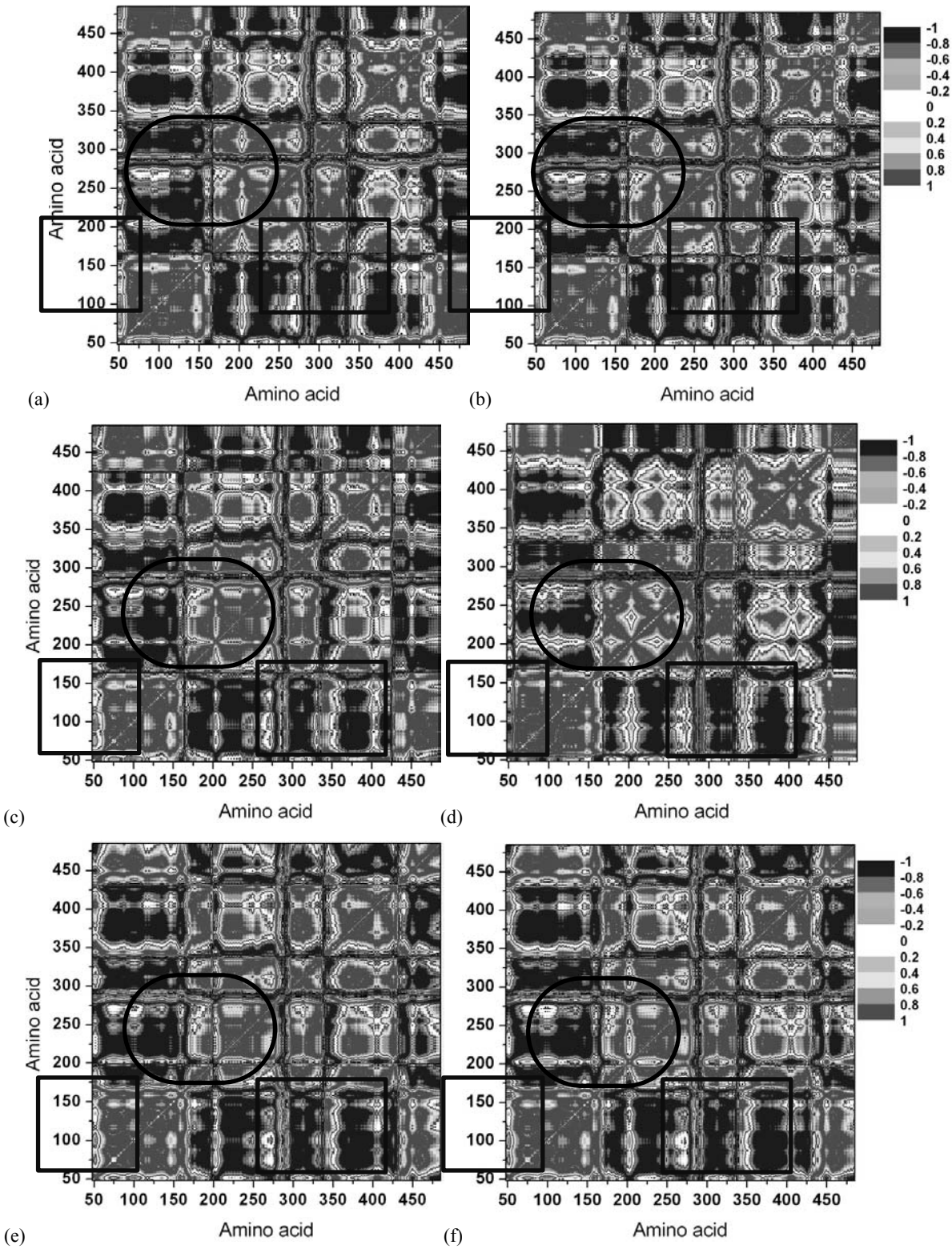

Fig. 3 – The covariance matrix of all Cα atoms pairs calculated for wt TPH2 (a), phosphorylated wt TPH2 (b), Pro206Ser TPH2 (c), phosphorylated Pro206Ser TPH2 (d), Arg441His TPH2 (e) and phosphorylated Arg441His TPH2 (f). The strongest positive correlations between residues (correlation values greater than 0.8) are represented with red and the strongest negative correlations (values smaller than -0.8) are represented with blue. Correlation values in the range of -0.2 up to 0.2 are considered insignificant and are represented with white. In all the plots, regions where mutations and phosphorylation change the positive correlation pattern are highlighted with circles and squares.

In wt TPH2, the motions of N-terminal regulatory domain (residues 48-164) are correlated with the motion of a C-terminal region (residues 433-485) that comprises the tetramerization domain (residues 458-485). Both regions are also positively correlated with residues 286-295 and 338-348 and anticorrelated with the remainder regions. Residues 167-283, comprising a cofactor binding region (residues 169-175), move in positive correlation with residues 297-336 and in negative correlation with residues 294-332 and 433-485. The two mutations, especially Arg441His, alter the strong positive or negative correlation between the tetramerization domain and the other regions. Also, new correlated motion regions appear on the covariance matrix of all Cα atoms pairs calculated for Pro206Ser TPH2 and Arg441His TPH2. For instance, in the case of Pro206Ser TPH2, the region 112-132 moves in positive correlation with 399-407. In the case of Arg441His TPH2, residues 60-162 move correlated with residues 198-207, residues 347-409 move correlated with residues 166-196 and residues 445-485 move correlated with residues 197-311.

In the case of wt TPH2 and Arg441His TPH2 phosphorylated monomers, the motions correlation pattern is similar to that of the unphosphorylated monomers. Significant differences are seen in the case of Pro206Ser TPH2. In the phoshorylated monomer, residues 58-148 move in positive correlation with residues 199-209. The region 263-277 moves almost independently from residues 260-280. Residues 331-350 move weakly correlated with the regulatory domain, while residues 332-338 move strongly correlated with residues 337-423.

CONCLUSIONS

We investigated the mechanism by which two mutations associated with the bipolar syndrome (Pro206Ser) and with major depression (Arg441His) alter the functionality of TPH2 by using molecular modeling techniques. The structural model of wt TPH2 monomer with catalytic sites comprising iron in the ferric state and three water molecules was built using homology modeling techniques. The optimization of the catalytic site geometry by quantum mechanics techniques produces a catalytic site conformation in which Fe^{3+} is found at similar distances from the protein and water atoms that coordinate it and forms ~90^{o} angles with them. Mutant and phosphorylated TPH2 monomers were built based on the QM/MM optimized wt TPH2 monomer model. By calculating the solvent accessible surface and solvation energy, we found that mutations widen the catalytic site and increase its solvation energy, and by that, altering the catalytic site ability to bind the substrates and co substrates. Upon phosphorylation at all the putative sites, the catalytic site surface and solvation energy increases in the case of wt TPH2 and Pro206Ser TPH2, while in the case of Arg441His TPH2 we observed a opposite effect. By analyzing wt and mutant TPH2 fluctuations in the slowest normal mode, we found that mutations enhance the flexibility of residues 50-67 from the regulatory domain. The increased flexibility in this area should contribute to the instability of mutant TPH2. Also, mutations increase the flexibility of the cofactor binding region (residues 169-175) and of two regions close to the loops that line the active site. By analyzing the covariance matrix between all Cα residue pairs of wt and mutant TPH2 monomers in the slowest normal mode, we found that mutations, especially Arg441His, alter the strong positive or negative correlation between the tetramerization domain and the other regions. Our results point toward a double effect of mutations on TPH2: on one hand, mutations alter the catalytic site electrostatic properties and on the other hand, alter the flexibility of key regions for enzyme functioning. The results obtained on phosphorylation influence on wt and mutant TPH2 monomers show that phosphorylations increase their flexibility. Our future work will focus on a systematic analysis of phosphorylated wt and mutant TPH2 in order determine the mechanism by which phosphorylations activate the enzyme.

REFERENCES

1. K. Tenner, D. Walther and M. Bader, *J. Neurochem.*, **2007**, *102*, 1887-94.
2. H. Meltzer, *Br. J. Psychiatry Suppl.*, **1989**, 25-31.
3. M. Abbar, P. Courtet, S. Amadeo, Y. Caer, J. Mallet, M. Baldy-Moulinier, D. Castelnau and A. Malafosse, *Arch. Gen. Psychiatry*, **1995**, *52*, 846-9.
4. J. J. Mann, V. Arango and M. D. Underwood, *Ann. N. Y. Acad. Sci.*, **1990**, *600*, 476-84; discussion 484-5.
5. J. J. Mann, K. M. Malone, D. A. Nielsen, D. Goldman, J. Erdos and J. Gelernter, *Am. J. Psychiatry*, **1997**, *154*, 1451-3.
6. I. Winge, J. A. McKinney, P. M. Knappskog and J. Haavik, *J. Neurochem.*, **2007**, *100*, 1648-57.
7. D. J. Walther, J. U. Peter, S. Bashammakh, H. Hortnagl, M. Voits, H. Fink and M. Bader, *Science*, **2003**, *299*, 76-76.

8. M. Grigoroiu-Serbanescu, C. C. Diaconu, S. Herms, C. Bleotu, J. Vollmer, T. W. Muhleisen, D. Prelipceanu, L. Priebe, R. Mihailescu, M. J. Georgescu, D. Sima, M. Grimberg, M. M. Nothen and S. Cichon, *Psychiatr. Genet.*, **2008**, *18*, 240-7.
9. S. Cichon, I. Winge, M. Mattheisen, A. Georgi, A. Karpushova, J. Freudenberg, Y. Freudenberg-Hua, G. Babadjanova, A. Van Den Bogaert, L. I. Abramova, S. Kapiletti, P. M. Knappskog, J. McKinney, W. Maier, R. A. Jamra, T. G. Schulze, J. Schumacher, P. Propping, M. Rietschel, J. Haavik and M. M. Nothen, *Hum. Mol. Genet.*, **2008**, *17*, 87-97.
10. N. Carkaci-Salli, J. M. Flanagan, M. K. Martz, U. Salli, D. J. Walther, M. Bader and K. E. Vrana, *J. Biol. Chem.*, **2006**, *281*, 28105-12.
11. M. S. Windahl, C. R. Petersen, H. E. Christensen and P. Harris, *Biochemistry*, **2008**, *47*, 12087-94.
12. L. Wang, H. Erlandsen, J. Haavik, P. M. Knappskog and R. C. Stevens, *Biochemistry*, **2002**, *41*, 12569-74.
13. K. D. Koehntop, J. P. Emerson and L. Que, Jr., *J. Biol. Inorg. Chem.*, **2005**, *10*, 87-93.
14. I. Winge, J. A. McKinney, M. Ying, C. S. D'Santos, R. Kleppe, P. M. Knappskog and J. Haavik, *Biochem. J.*, **2008**, *410*, 195-204.
15. H. Molina, D. M. Horn, N. Tang, S. Mathivanan and A. Pandey, *Proc. Natl. Acad. Sci. U. S. A.*, **2007**, *104*, 2199-204.
16. P. Zill, T. C. Baghai, P. Zwanzger, C. Schule, D. Eser, R. Rupprecht, H. J. Moller, B. Bondy and M. Ackenheil, *Mol. Psychiatry*, **2004**, *9*, 1030-6.
17. X. Zhang, R. R. Gainetdinov, J. M. Beaulieu, T. D. Sotnikova, L. H. Burch, R. B. Williams, D. A. Schwartz, K. R. Krishnan and M. G. Caron, *Neuron.*, **2005**, *45*, 11-6.
18. S. F. Altschul, T. L. Madden, A. A. Schaffer, J. Zhang, Z. Zhang, W. Miller and D. J. Lipman, *Nucleic Acids Res.*, **1997**, *25*, 3389-402.
19. B. Kobe, I. G. Jennings, C. M. House, B. J. Michell, K. E. Goodwill, B. D. Santarsiero, R. C. Stevens, R. G. Cotton and B. E. Kemp, *Nat. Struct. Biol.*, **1999**, *6*, 442-8.
20. F. Fusetti, H. Erlandsen, T. Flatmark and R. C. Stevens, |*J. Biol. Chem.*, **1998**, *273*, 16962-7.
21. K. E. Goodwill, C. Sabatier, C. Marks, R. Raag, P. F. Fitzpatrick and R. C. Stevens, *Nat. Struct. Mol. Biol.*, **1997**, *4*, 578-585.
22. A. Sali and T. L. Blundell, *J. Mol. Biol.*, **1993**, *234*, 779-815.
23. H. Erlandsen, F. Fusetti, A. Martinez, E. Hough, T. Flatmark and R. C. Stevens, *Nat. Struct. Biol.*, **1997**, *4*, 995-1000.
24. B. R. E. Brooks B. R. , S. D. J. Olafson B. D. , Swaminathan S. and Karplus M. , *J. Comp. Chem.*, **1983**, *4*, 187-217.
25. M. W. Schmidt, K. K. Baldridge, J. A. Boatz, S. T. Elbert, M. S. Gordon, J. H. Jensen, S. Koseki, N. Matsunaga, K. A. Nguyen, S. J. Su, T. L. Windus, M. Dupuis and J. A. Montgomery, *J. Comp. Chem.*, **1993**, *14*, 1347-1363.
26. A. D. MacKerell, D. Bashford, M. Bellott, R. L. Dunbrack, J. D. Evanseck, M. J. Field, S. Fischer, J. Gao, H. Guo, S. Ha, D. Joseph-McCarthy, L. Kuchnir, K. Kuczera, F. T. K. Lau, C. Mattos, S. Michnick, T. Ngo, D. T. Nguyen, B. Prodhom, W. E. Reiher, B. Roux, M. Schlenkrich, J. C. Smith, R. Stote, J. Straub, M. Watanabe, J. Wiorkiewicz-Kuczera, D. Yin and M. Karplus, *J. Phys. Chem. B*, **1998**, *102*, 3586-3616.
27. M. M. Tirion, *Phys. Rev. Lett.*, **1996**, *77*, 1905-1908.
8. W. Im, D. Beglov and B. Roux, *Comp. Phys. Comm.*, **1998**, *111*, 59-75.
29. M. Schapira, M. Totrov and R. Abagyan, *J. Mol. Recognit.*, **1999**, *12*, 177-90.
30. D. Rodriguez-Larrea, B. Ibarra-Molero and J. M. Sanchez-Ruiz, *Biophys. J.*, **2006**, *91*, L48-50.
31. E. Balog, M. Laberge and J. Fidy, *Biophys. J.*, **2007**, *92*, 1709-16.